Contribution from the Chemistry Department, State University of New York at Buffalo, Buffalo, New York 14214, and the Laboratoire de Chimie Quantique, Institut LeBel, Université Louis Pasteur, 67000 Strasbourg, France

Experimental and Theoretical Electron Density Analysis of Metal-Metal Bonding in Dichromium Tetraacetate

M. BENARD,[1a] P. COPPENS,*[1b] M. L. DeLUCIA,[1b] and E. D. STEVENS[1b]

Received October 30, 1979

The electron deformation density in dichromium tetraacetate has been obtained from low-temperature X-ray diffraction data and from theoretical wave functions at the Hartree-Fock, unrestricted Hartree-Fock, and limited configuration interaction levels. The experimental determination of the dihydrate at 90 K (space group $C2/c$, a = 13.121 (2) Å, b = 8.575 (1) Å, c = 13.856 (2) Å, β = 116.737 (2)°, Z = 4) shows a contraction of the Cr-Cr bond to 2.3532 (4) Å compared with the room-temperature value of 2.362 (1) Å and gives deformation densities which after averaging over chemically equivalent regions show a broad region of excess electron density off the Cr-Cr bond axis and an electron-deficient area along this axis. Though the SCF configuration is strongly bonding in the Cr-Cr region, the corresponding theoretical deformation density functions do not display sharp peaks, a result attributed to the diffuse character of the interacting d orbitals. The UHF and CI deformation maps show even less density in the Cr-Cr region, as may be expected from the corresponding overlap populations which are 0.64 and 0.08 e for the SCF and UHF configurations, respectively. The CI map is in many respects similar to the experimental functions. Some discrepancies observed near the center of the molecule are tentatively attributed to the presence of axial ligands in the experimental determination.

Introduction

The continuous transition from moderately sized metal cluster compounds to infinite arrays of metal atoms is of interest as bonding in metals is generally conceived as being of a different nature than covalent bonding in molecules. As part of a program to study this interface between molecular and metallic bonding by accurate diffraction techniques, we report here an experimental electron density analysis of dichromium tetraacetate dihydrate. The results are compared with theoretical electron density maps obtained from three different types of wave functions, two of which include part of the correlation effects. Earlier experimental studies concerned the bonding in beryllium and vanadium metal[2] and in the alloy V_3Si,[3] while analyses on $Co_2(CO)_8$ and $Co_3(CO)_9CH$ are presently in progress.

The structure of dichromium tetraacetate dihydrate was first investigated by Van Niekerk, Schoening, and deWet,[4] who reported it to be a binuclear molecule isostructural with copper acetate and to have a Cr-Cr distance of 2.64 Å. However, a reinvestigation by Cotton et al.[5] showed the bond to be considerably shorter. Its length of 2.362 (1) Å is less than the interatomic distance in the metal and comparable with the separation in the one-dimensional chromium atom chain in Cr_3Si in which a strong covalent interaction is thought to exist.

Cotton and co-workers subsequently discovered considerably shorter bonds in compounds such as $Cr_2(DMP)_4$ (DMP = 2,6 dimethoxyphenyl) in which the bond length is 1.847 (1) Å,[6] while the bond is also somewhat shorter in the anhydrous chromous acetate (2.280 (2) Å).[7] Theoretical calculations indicate the electronic effect which causes the variability of the Cr-Cr bond to be greatly magnified by the shallowness of the interatomic potential in these compounds.[8] This interpretation is also supported by the length of 2.280 (2) Å of the formally triple bond in bis(dicarbonyl(pentamethylcyclopentadienyl)chromium), $[\pi\text{-}(CH_3)_5C_5Cr(CO)_2]_2$,[9] a length comparable to that of the formally quadruple bond in chromous acetate, and by the lack of a clear correlation between the length of the Cr-Cr quadruple bond and the distance to axial ligand atoms.[10]

Preliminary results of the experimental study have been reported elsewhere.[11]

Table I. Crystallographic Data for $Cr_2(O_2CCH_3)_4 \cdot 2H_2O$

1. Unit Cell Data

molecular mass: 376.23 daltons
space group: $C2/c$
cell dimens: a = 13.121 (2) Å, b = 8.575 (1) Å, c = 13.856 (2) Å, β = 116.737 (2)°, Z = 4, ρ(X-ray) = 1.795 g/cm³ for 90 K; a = 13.123 (3) Å, b = 8.589 (2) Å, c = 13.867 (3) Å, β = 116.689 (2)°, Z = 4, ρ(X-ray) = 1.789 g/cm³ for 120 K; a = 13.211 (6) Å, b = 8.617 (3) Å, c = 13.962 (5) Å, β = 116.85 (3)°, Z = 4, ρ(X-ray) = 1.762 g/cm³ for room temperature[a]

2. Data Collection

	data set I	data set II
no. of reflctns measd excluding stds	20815	6103
no. of unique reflctns	5885	2103
$\Sigma\lvert F_o^2 - \langle F_o^2\rangle\rvert/\Sigma F_o^2$	0.021,[b] 0.043[c]	0.033
$F(000)$	192	

[a] Reference 5. [b] $(\sin\theta)/\lambda < 0.54$ Å^{-1}. [c] $(\sin\theta)/\lambda > 0.54$ Å^{-1}.

Experimental Section

Crystals of dichromium tetraacetate dihydrate were prepared by D. F. Chodosh following a synthesis described in the literature.[12]

Two sets of single-crystal X-ray data were collected on an automated Picker four-circle diffractometer at 90 and 120 K, respectively, using Nb filtered Mo Kα radiation (λ = 0.7107 Å) and the self-regulating CT-38 X-ray cryostat.[13] Unit cell dimensions at the two temperatures were determined by least-squares refinement of the setting angles of 29 carefully centered reflections with $60.0 < 2\theta < 65.0°$ and are listed together with other crystallographic information in Table I. Both

(1) (a) Université Louis Pasteur. (b) State University of New York.
(2) Coppens, P. *Int. Phys. Conf. Ser.* **1978**, *39*, 630.
(3) Staudenmann, J. L.; Coppens, P.; Muller, F. *Solid State Commun.* **1976**, *19*, 29.
(4) Van Niekerk, N. J.; Schoening, F. R. F.; deWet, J. F. *Acta Crystallogr.* **1953**, *6*, 501.
(5) Cotton, F. A.; DeBoer, B.; LaPrade, M.; Pipal, J.; Ucko, D. *Acta Crystallogr., Sect. B* **1971**, *27*, 1664.
(6) Cotton, F. A. *Acc. Chem. Res.* **1978**, *11*, 225. Cotton, F. A., Koch, S.; Millar, M. *J. Am. Chem. Soc.* **1977**, *99*, 7372.
(7) Cotton, F. A.; Rice, C.; Rice, G. *J. Am. Chem. Soc.* **1977**, *99*, 4704.
(8) Benard, M. *J. Am. Chem. Soc.* **1978**, *100*, 2354.
(9) Potenza, J.; Giordano, P.; Mastropaolo, D.; Efraty, A. *Inorg. Chem.* **1974**, *13*, 2540.
(10) Cotton, F. A.; Extine, M. W.; Rice, G. W. *J. Am. Chem. Soc.* **1978**, *17*, 176.
(11) DeLucia, M. L.; Stevens, E. D.; Coppens. P. *ACA Abstr.* **1976**, [2] *4* (2), 61. DeLucia, M. L. Thesis, State University of New York at Buffalo, Buffalo, N.Y.
(12) Hin, F.; Herzog, S. In "Handbook of Preparative Inorganic Chemistry", Brauer, G., Ed.; Academic Press: London, 1965; Vol. II, p 1368.
(13) Coppens, P.; Ross, F.; Blessing, R.; Cooper, W. F.; Larsen, F. K.; Leipoldt, J.; Rees, B.; Leonard, R. *J. Appl. Crystallogr.* **1974**, *7*, 315.

0020-1669/80/1319-1924$01.00/0

Table II. Final Agreement Factors[a]

	NO	NV	G	R(F)	$R_w(F)$	$R(F^2)$	$R_w(F^2)$
b	4989	124	1.65	0.026	0.031	0.045	0.062
c	3570	91	1.19	0.024	0.025	0.038	0.050
d	3626	124	2.72	0.054	0.030	0.053	0.058

[a] $G = [\Sigma w\Delta^2/(NO - NV)]^{1/2}$, $R(F) = \Sigma||F_o| - |F_c||/\Sigma|F_o|$, $R_w(F) = [\Sigma w(|F_o| - |F_c|)^2/\Sigma wF_o^2]^{1/2}$, and corresponding expressions for F^2. NO = number of observations; NV = number of variables. [b] Full data refinement of data set I. [c] Refinement of data above 0.65 $Å^{-1}$ for data set I. [d] Full data refinement of data set II.

data sets were collected on the same crystal of approximate dimensions 0.23 × 0.18 × 0.18 mm and a volume of 5.92×10^{-3} mm^3. Data were collected in the θ–2θ step scan mode up to $2\theta = 122°$ (set I) and $2\theta = 75°$ (set II). Of each form {hkl} at least two symmetry-related reflections were measured. The full reflection profiles were analyzed as described previously.[14] Lorentz–polarization factors were applied, and an absorption correction was made ($\mu = 15.67$ cm^{-1}) by using the Gaussian integration method. The transmission factor varied between 0.75 and 0.81. Details on averaging of symmetry-equivalent relections are given in Table I.

Least-Squares Refinements. Positional and thermal parameters from Cotton et al.[5] were used as a starting set in a least-squares minimization of $\sum w(F_o^2 - k^2F_c^2)^2$, where $1/w = \sigma^2 = \sigma^2_{counting} + (0.02F_o^2)^2$. Scattering factors and anomalous dispersion were as listed in the "International Tables for X-ray Crystallography", except for the hydrogen atom for which the contracted-atom values of Stewart, Davidson, and Simpson[15] were used. Reflections with $F_o^2 < 3\sigma(F_o^2)$ were included in the refinement only when $F_c^2 < F_t = 3\sigma(F_o^2)$, in which case F_o^2 was replaced by F_t. Refined parameters include positional parameters, anisotropic thermal parameters for all nonhydrogen atoms, isotropic parameters for the hydrogen atoms, and a scale and an isotropic extinction parameter. Both data sets were treated separately as data collection temperatures were different. For set I a high-order refinement ($\sin\theta/\lambda > 0.65$ $Å^{-1}$) was also performed varying all but the hydrogen and extinction parameters. Agreement factors are given in Table II, while final parameters from data set I are listed in Table III.

Deformation density maps calculated after completion of the refinement of data set I contain two relatively large peaks in the Cr–Cr′–C(1) plane at almost equal distance but opposite directions from the chromium atom. The peaks have a height of 0.6 e $Å^{-3}$, and their maxima are located at (0.042 89, 0.076 36, −0.042 14) and (−0.047 48, −0.072 45, 0.039 71) at 0.86 and 0.58 Å from the chromium atoms (Figure 2).

As no corresponding maxima are observed in the chemically equivalent plane through the Cr–Cr′ bond and the second acetate molecule, there is no obvious chemical explanation for these maxima, a conclusion which prompted the collection of the second data set. However, the deformation density from this second set shows identical features, indicating that the effect is unlikely to be due to a small subset of erroneous reflections. In search of other possible explanations for the observation an acentric refinement in space group *Cc* was performed, which failed to give improved agreement between calculated and observed structure factors and suffered from very high parameter correlations. A number of disordered models were also investigated, including one with (for chromium) $x'' = -z$, $y'' = y$, and $z'' = -x$, a transformation chosen because it places the Cr″ atom approximately at one of the extraneous peaks which would allow the original Cr atom to move in the direction of the second peak (note that the **a** and **c** identity translations have almost identical lengths). The refinement of the disordered model was constrained so that both sets of Cr atoms would have identical geometries. This disordered model converged extremely slowly and did not seem to lead to an improved fit to the data.

An alternative and more likely explanation for the residual peaks is anharmonicity of the thermal motion of the Cr atoms which would show up preferentially near the relatively heavy transition-metal atom. Examination of the packing diagrams indicates that the peaks are displaced from the Cr atoms in the directions of voids in the crystal, so that the potential for molecular motion in these directions may indeed be shallower near the equilibrium position than would be predicted by an harmonic model.

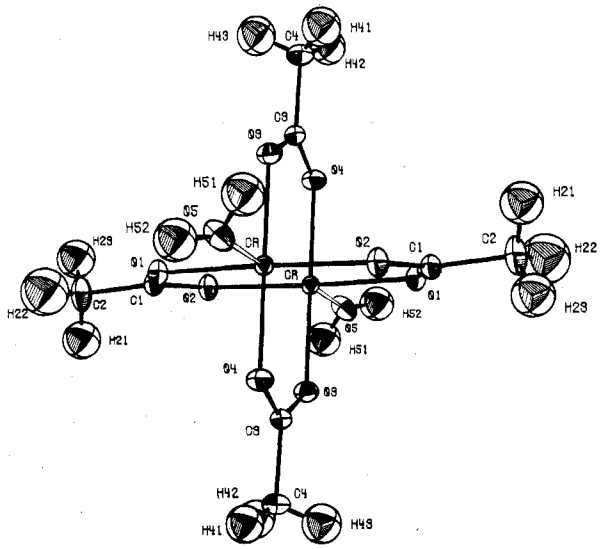

Figure 1. 75% Thermal probability ellipsoids at 90 K.

A subsequent refinement on the high-order data ($(\sin\theta)/\lambda > 0.75$ $Å^{-1}$) including third and fourth cumulants in the temperature factor formalism[16] gave a statistically significant improvement in *R* factors but failed to remove the satellite peaks in the difference maps calculated with all data. Further analysis showed that these peaks originate mainly from low-order reflections. Though this does not exclude the possibility of an anharmonic potential curve, it complicates analysis of their origin, as low-order reflections are also influenced by the anisotropy of the bonding around the chromium atoms. Collection of neutron diffraction data would allow distinction between thermal and bonding effects. However, it may not be feasible to grow good-quality neutron-diffraction size crystals of this compound.

Molecular Orbital Calculations. The theoretical density maps were obtained from ab initio LCAO–MO–SCF calculations on $Cr_2(O_2CH)_4$ carried out with the ASTERIX system of programs.[17] The Gaussian basis sets were (11,7,5) for Cr, (8,4) for the first row atoms, and (4) for hydrogen, contracted to a minimum basis set for the inner shells and the 4s and 4p shells of the chromium atoms but a split set for the valence shells. The Cr–Cr distance was taken equal to 2.362 Å. The symmetry-adapted RHF closed-shell configuration corresponding to the quadruply bonded $\sigma^2\pi^4\delta^2$ configuration (hereafter referred to as SCF) has an energy of −2833.717 au. A configuration interaction expansion was performed including the $\sigma^2\pi^4\delta^2$ configuration as the leading term. This configuration interacts either directly or indirectly with the set of 15 configurations corresponding to one or several excitations of the type $a^2 \rightarrow a^{*2}$, where a denotes one of the four types of σ, π, and δ orbitals and a* the corresponding antibonding orbital.[8,18] The wave function associated with this development will be referred to as CI. The associated energy is −2834.401 au.

On the other hand, it has been shown that for multiply bonded complexes, the symmetry adapted RHF ground-state configuration may not be the one-determinant configuration of lowest energy. A one-determinant wave function including part of the correlation energy can be obtained by removing either the space-symmetry constraints alone or both spin- and space-symmetry constraints.[19,20] In the case of $Cr_2(O_2CH)_4$, the one-determinant wave function of lowest energy very probably corresponds to a spin-unrestricted wave-function for which the constraint induced by the mirror plane of symmetry between the metal atoms has been removed. The energy associated with this

(14) Blessing, R. H.; Coppens, P.; Becker, P. *J. Appl. Crystallogr.* **1974**, *7*, 488.
(15) Stewart, R. F.; Davidson, E. R.; Simpson, W. T. *J. Chem. Phys.* **1965**, *42*, 3175.
(16) Johnson, C. K. *Acta Crystallogr., Sect. A* **1969**, *25*, 187.
(17) Benard, M.; Dedieu, A.; Demuynck, J.; Rohmer, M.-M.; Strich, A.; Veillard, A. "ASTERIX"., a system of programs for the Univac 1110, unpublished work. Benard, M. *J. Chim. Phys. Phys.-Chim. Biol.* **1976**, *73*, 413.
(18) Benard, M.; Weillard, A. *Nouv. J. Chim.* **1976**, *1*, 97.
(19) Noodleman, L.; Norman, J. G. *J. Chem. Phys.* **1979**, *70*, 4903.
(20) Benard, M. *J. Chem. Phys.* **1979**, *71*, 2546.

Table III. Atomic Coordinates from Refinement of All Data (Thermal Parameters in Å^2, $\times 10^5$ for Cr, $\times 10^4$ for O and C, and $\times 10^3$ for H)

atom	x	y	z	U_{11}	U_{22}	U_{33}	U_{12}	U_{13}	U_{23}
Cr	0.045 09 (1)	0.074 57 (2)	−0.041 02 (1)	566 (4)	634 (3)	593 (3)	−23 (4)	269 (2)	−23 (4)
O(1)	0.186 18 (5)	0.088 13 (8)	0.104 02 (5)	73 (2)	107 (2)	74 (2)	−11 (2)	29 (1)	4 (2)
O(2)	0.102 15 (6)	−0.059 87 (8)	0.180 42 (5)	78 (2)	109 (3)	73 (2)	−17 (2)	26 (1)	7 (1)
O(3)	−0.097 72 (6)	0.127 83 (9)	0.077 78 (5)	100 (2)	86 (2)	118 (2)	−1 (2)	63 (2)	−10 (2)
O(4)	−0.009 70 (6)	0.268 80 (8)	0.001 36 (5)	105 (2)	78 (2)	116 (2)	6 (2)	65 (2)	−2 (2)
O(5)	0.127 12 (7)	0.204 36 (9)	−0.129 91 (6)	165 (3)	129 (3)	123 (2)	−64 (2)	97 (2)	−37 (2)
C(1)	0.185 85 (7)	0.021 87 (10)	0.185 94 (6)	75 (3)	96 (3)	72 (2)	−2 (2)	25 (2)	−1 (2)
C(2)	0.286 78 (9)	0.040 91 (15)	0.294 53 (7)	106 (3)	209 (4)	87 (2)	−46 (3)	8 (2)	6 (2)
C(3)	−0.068 05 (7)	0.257 26 (10)	0.053 55 (6)	71 (2)	81 (2)	90 (2)	7 (2)	29 (2)	−11 (2)
C(4)	−0.105 20 (9)	0.404 67 (11)	0.087 08 (8)	130 (3)	100 (3)	158 (3)	20 (2)	67 (3)	−32 (2)

atom	x	y	z	U	atom	x	y	z	U
H(21)	0.260 (2)	0.092 (2)	0.342 (2)	29 (5)	H(42)	−0.067 (1)	0.494 (2)	0.082 (1)	23 (5)
H(22)	0.339 (2)	0.101 (2)	0.290 (2)	44 (7)	H(43)	−0.180 (2)	0.413 (2)	0.052 (2)	27 (5)
H(23)	0.318 (2)	−0.063 (2)	0.325 (2)	30 (6)	H(51)	0.119 (2)	0.165 (2)	−0.190 (1)	27 (5)
H(41)	−0.093 (1)	0.390 (2)	0.161 (1)	27 (5)	H(52)	0.181 (1)	0.262 (2)	−0.115 (1)	26 (5)

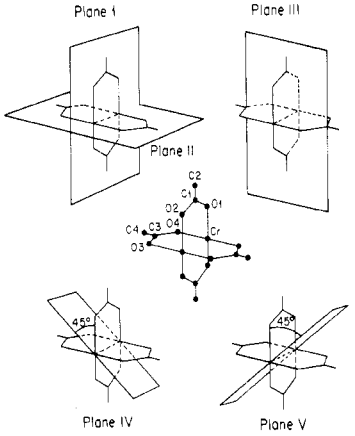

Figure 2. Definition of molecular planes.

UHF broken symmetry (BS) wave function is −2834.652 au.

Deformation density maps for the planes I ≡ II and IV ≡ V have been computed from the SCF, CI, and BS wave functions and are displayed in Figures 7a–c and 8a–c respectively.

Discussion

Molecular Dimensions and Vibrational Parameters. As expected the thermal parameters of the second set are larger than those for set I, the average ratios of the diagonal tensor elements being 1.46, 1.47, and 1.57 for U_{11}, U_{22} and U_{33}, respectively, which is slightly larger than the ratio of the data collection temperatures. Since positional parameters from the two data sets show no significant differences, the more accurate bond lengths based on set I have been listed in Table IV. Thermal probability ellipsoids from set I are shown in Figure 1.

The Cr–Cr distance at low temperature of 2.353 (1) Å is 0.01 Å less than the value reported from the room-temperature study (2.362 (1) Å). This relatively large contraction of an intramolecular bond length is in agreement with the shallowness of the Cr–Cr potential predicted by theoretical calculations.[8]

The Cr–O(acetate) distances are all within 0.02 Å from the average value of 2.021 (1) Å, while the axial Cr–O(water) distance is 2.260 (1) Å. C–C and C–O bond lengths in the acetate ligand are as observed in other complexes.

Experimental Deformation Density Maps. Deformation densities defined as

$$\Delta\rho = \rho_{obsd} - \rho_{calcd}(HO)$$

(where $\rho_{calcd}(HO)$ is the density calculated from high-order parameters and spherical atom form factors) were calculated in the planes defined in Figure 2. Only the more accurate densities based on data set I are discussed here. The maps

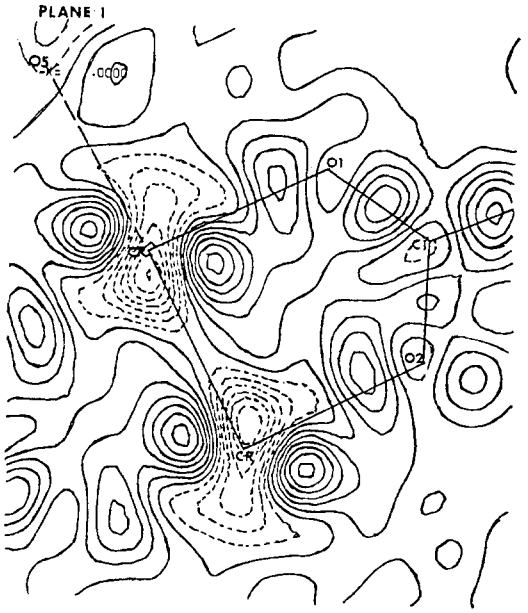

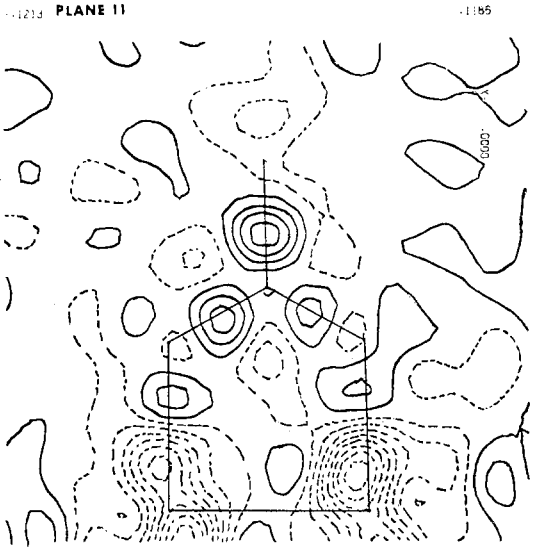

Figure 3. Deformation density for planes I and II. Contours are at 0.10 e Å^{-3}, and negative contours are broken.

shown in Figures 2–5 includes all data up to $(\sin\theta)/\lambda = 0.65$ Å^{-1}. Maps including data beyond the limit suffer from an increase in the noise level due to contributions from large numbers of high-order reflections but show no change in the density features discussed below. Such noise may be elimi-

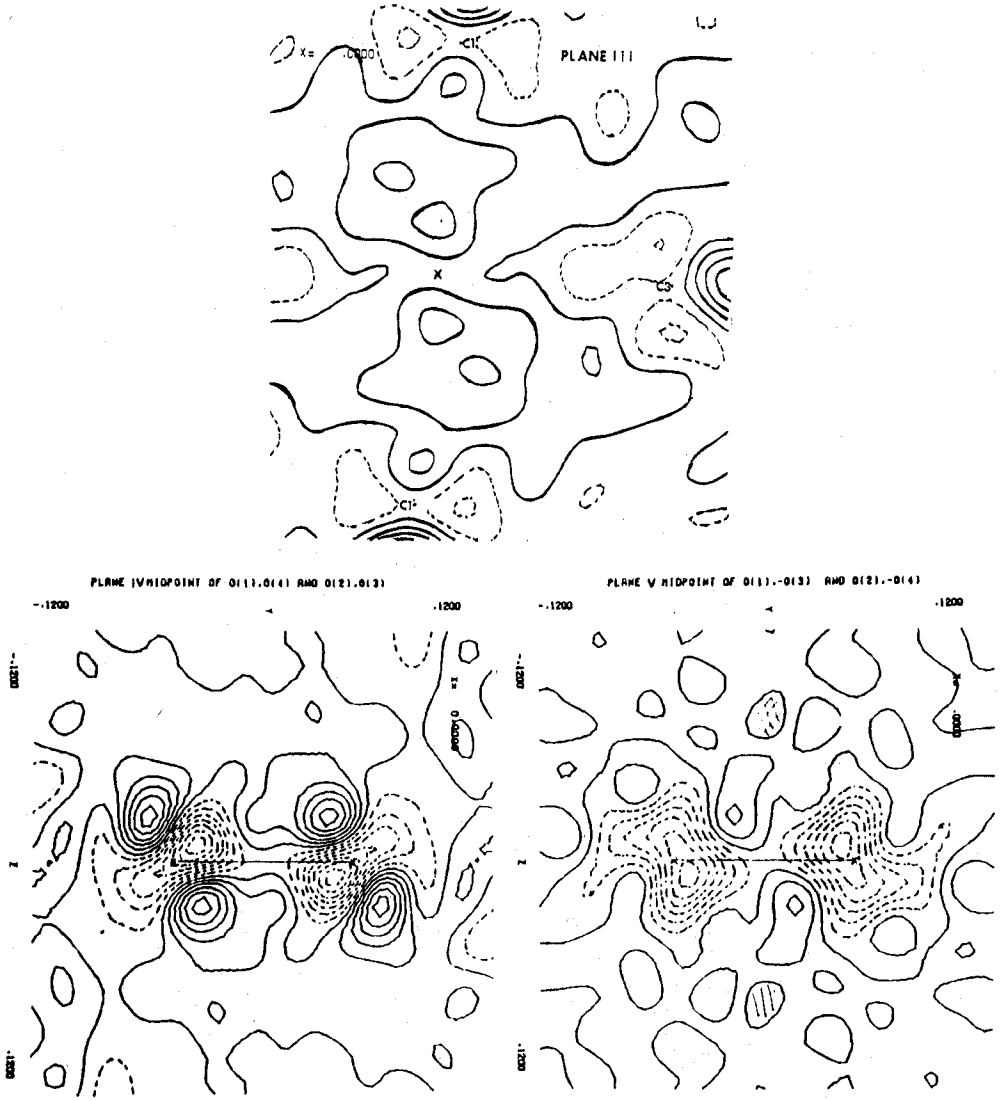

Figure 4. Same as Figure 3 but for planes III, IV, and V.

nated in model density maps on the basis of results of a refinement with aspherical atom density functions, as done for example in the case of *p*-nitropyridine *N*-oxide[21] and FeS_2.[22] Due to computer time limitations, no such refinement has been performed for binuclear complexes.

The most prominent features in plane I are the two density peaks of 0.6 e $Å^{-3}$ in the neighborhood of the Cr atoms discussed above, which are absent in the chemically equivalent plane II. Peaks of height 0.2–0.4 e $Å^{-3}$ are found in all four Cr–O(acetate) bonds, while density also accumulates between the oxygen and carbon (ρ_{max} = 0.1–0.3 e $Å^{-3}$) and between the two adjacent carbon atoms ($\rho_{max} \approx 0.4$ e $Å^{-3}$). Excess electron density is also observed in the lone-pair regions at the back of the acetate oxygen atoms. No density is found in the bonds in the water molecule because of the lack of accurate information on the positions of the hydrogen nuclei. We note that an analysis of the density in regions surrounding hydrogen atoms in general requires the availability of neutron diffraction data.

For a study of the density in the Cr–Cr region, chemically equivalent planes I and II and planes IV and V were averaged. Further "left–right" averaging permitted by the D_{4h} (4*mm*) symmetry of the complex gave the density maps reproduced in Figures 5 and 6 which clearly show density in bond and lone-pair regions of the acetate group and in the Cr–O bonds but conspicuously lack electron density in the σ-bond region between the Cr atoms.

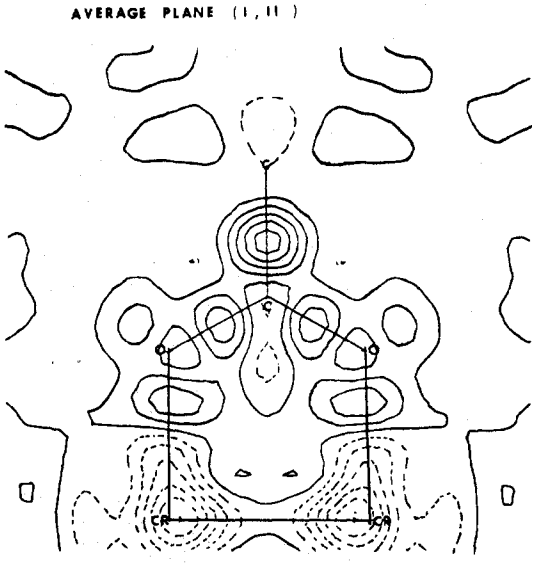

Figure 5. Average of planes I and II. Contours are as in Figure 3.

(21) Hansen, N. K.; Coppens, P. *Acta Crystallogr., Sect. A* **1978**, *34*, 909.
(22) Stevens, E. D.; Coppens, P. *Acta Crystallogr., Sect. A* **1979**, *35*, 536.

Table IV

Interatomic Distances (Å) and Angles (Deg)

	a	*b*
1. Intramolecular Bond Distances		
Cr–Cr′	2.3532 (4)	2.362 (1)
Cr–O(5)	2.2598 (8)	2.272 (3)
Cr–O(1)	2.0327 (7)	2.030 (2)
Cr–O(2)	2.0301 (8)	2.031 (2)
Cr–O(3)	2.0162 (7)	2.009 (2)
Cr–O(4)	2.0039 (7)	2.001 (2)
C(1)–O(1)	1.271 (1)	1.263 (4)
C(1)–O(2)	1.276 (1)	1.268 (4)
C(3)–O(3)	1.270 (1)	1.266 (3)
C(3)–O(4)	1.272 (1)	1.262 (4)
C(1)–C(2)	1.501 (1)	1.488 (4)
C(3)–C(4)	1.502 (1)	1.492 (5)
O(5)–H(51)	0.86 (2)	0.79 (4)
O(5)–H(52)	0.80 (2)	0.70 (4)
C(2)–H(21)	0.97 (2)	0.89 (6)
C(2)–H(22)	0.85 (2)	0.80 (4)
C(2)–H(23)	0.99 (2)	0.97 (5)
C(4)–H(41)	0.97 (2)	0.89 (5)
C(4)–H(42)	0.93 (2)	0.87 (5)
C(4)–H(43)	0.88 (2)	0.84 (5)
2. Bond Angles		
Cr–Cr′–O(3)	87.59 (2)	87.32 (4)
Cr′–Cr–O(4)	89.17 (3)	88.80 (5)
Cr′–Cr–O(1)	89.18 (3)	88.76 (5)
Cr–Cr′–O(2)	87.47 (3)	87.27 (5)
Cr′–O(2)–C(1)	121.07 (5)	121.2 (2)
Cr′–O(3)–C(3)	120.33 (6)	120.7 (2)
Cr–O(4)–C(3)	119.28 (6)	119.7 (1)
Cr–O(1)–C(1)	119.33 (6)	119.9 (1)
O(1)–C(1)–O(2)	122.74 (7)	122.7 (1)
O(3)–C(3)–O(4)	123.55 (8)	123.4 (2)
O(1)–C(1)–C(2)	119.39 (8)	119.4 (2)
O(2)–C(1)–C(2)	117.87 (8)	117.8 (2)
O(3)–C(3)–C(4)	118.19 (7)	118.4 (2)
O(4)–C(3)–C(4)	118.21 (8)	118.2 (2)
O(1)–Cr–O(5)	93.75 (3)	93.97 (9)
O(2)–Cr–O(5)	89.70 (3)	90.08 (9)
O(3)–Cr–O(5)	89.14 (3)	89.15 (8)
O(4)–Cr–O(5)	94.13 (3)	94.75 (8)
O(1)–Cr–O(4)	87.13 (3)	87.57 (6)
O(1)–Cr–O(3)	92.06 (3)	91.84 (8)
O(4)–Cr–O(2)	90.98 (3)	90.88 (8)
O(2)–Cr–O(3)	89.64 (3)	89.44 (6)
Cr′–Cr–O(5)	175.67 (2)	175.61 (11)
O(1)–Cr–O(2)	176.18 (3)	175.76 (10)
O(4)–Cr–O(3)	176.67 (3)	176.08 (10)

Dihedral Angle[a] between Planes Defined by Cr–Cr′–C(1)′ and Cr–Cr′–C(3): 86.94 (3)°

Molecular Planes[a]

plane I: Cr, O(1), O(2), O(5), C(1)
$5.966x - 7.4222y - 5.3833z = 0.063\,4$

plane II: Cr, O(3), O(4), O(5), C(3)
$6.440x + 2.6500y + 7.5070z = 0.007\,87$

Distances (Å) of Atoms from Plane

plane I		plane II	
Cr	0.0012 (1)	Cr	0.0034 (1)
O(1)	−0.0340 (7)	O(3)	−0.0402 (7)
O(2)	−0.0217 (7)	O(4)	−0.0243 (7)
O(5)	0.0075 (9)	O(5)	−0.0839 (8)
C(1)	0.0153 (8)	C(3)	0.0103 (7)

[a] Based on parameters from the full data refinement of data set I. [b] Reference 5.

According to the 18-electron rule the bond between the two chromium atoms would have π and δ in addition to σ components. The maps indeed show a large area of excess electron density off the bond axis, which extends from the average of planes I and II (which is the π-bonding region) into the δ-bonding regions of planes IV and V (Figure 4). The standard deviation of the averaged density at general positions away from the immediate vicinity of the atoms is estimated at 0.02 e Å^{-3}. Density maxima of more than 0.10 e Å^{-3} which occur in the averaged planes are therefore significant and may be interpreted as evidence for the existence of δ and π bonding between the Cr atoms.

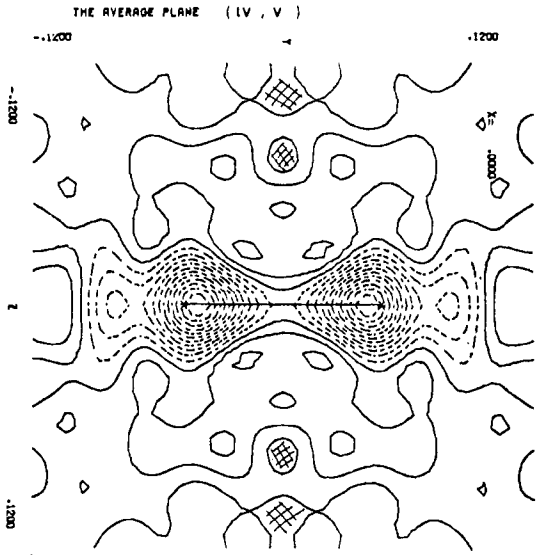

Figure 6. Average of planes IV and V. Contours are at 0.05 e Å^{-3}, and negative contours are broken.

Analysis of the Theoretical Maps and Comparison with Experiment. The three computed maps obtained from the SCF, CI, and BS wave functions are nearly identical in the region of the Cr–O and O–C–O bonds. The localization of the density peaks along these bonds and in the region of the oxygen lone pair is in agreement with the picture obtained from diffraction techniques. As has been noted previously, both electron accumulation and deficiencies are often found larger by the calculation than by the experiment, as thermal motion and limited resolution reduce the sharpest features in the experimental maps.[23] Quantitative discrepancies are also expected to arise from the lack of flexibility of the double-ζ basis set used for valence shells in the theoretical calculation.[24]

The similarity between SCF and CI maps around the metal atoms and in the region of the metal–metal bond might appear more surprising, considering the very large energy difference between the wave functions and the very small weight (18%) of the SCF strongly bonded configuration in the CI expansion. The large contributions of antibonding Cr–Cr orbitals tend in this case to annihilate the strength of the quadruple bond so that a formal bond order considerably less than four could be derived from this wave function (see, for instance, Cristoph and Koh).[25] However, the map obtained from the SCF wave function only exhibits a large, diffuse, and continuous accumulation zone over the σ- and π-bonding regions culminating at the center of symmetry of the system with a peak of 0.2 e Å^{-3} (Figure 7a). It is remarkable that this strongly bonded configuration does not generate any sharp peak in the bonding region. Such an absence of prominent features may be at-

(23) Stevens, E. D.; Rys, J.; Coppens, P. *Acta Crystallogr., Sect. A* **1977**, *33*, 333. Coppens, P.; Stevens, E. D. *Isr. J. Chem.* **1977**, *16*, 175. Rees, B.; Mitschler, A. *J. Am. Chem. Soc.* **1976**, *98*, 7918.
(24) Jones, D. S.; Pautler, D.; Coppens, P. *Acta Crystallogr., Sect. A* **1972**, *28*, 635. Smith, P. R.; Richardson, J. W. *J. Phys. Chem.* **1967**, *71*, 924. Bicerano, J.; Marynick, D. S.; Lipscomb, W. N. *J. Am. Chem. Soc.* **1978**, *100*, 732.
(25) Cristoph, G. G.; Koh, Y. B. *J. Am. Chem. Soc.* **1979**, *101*, 1422.

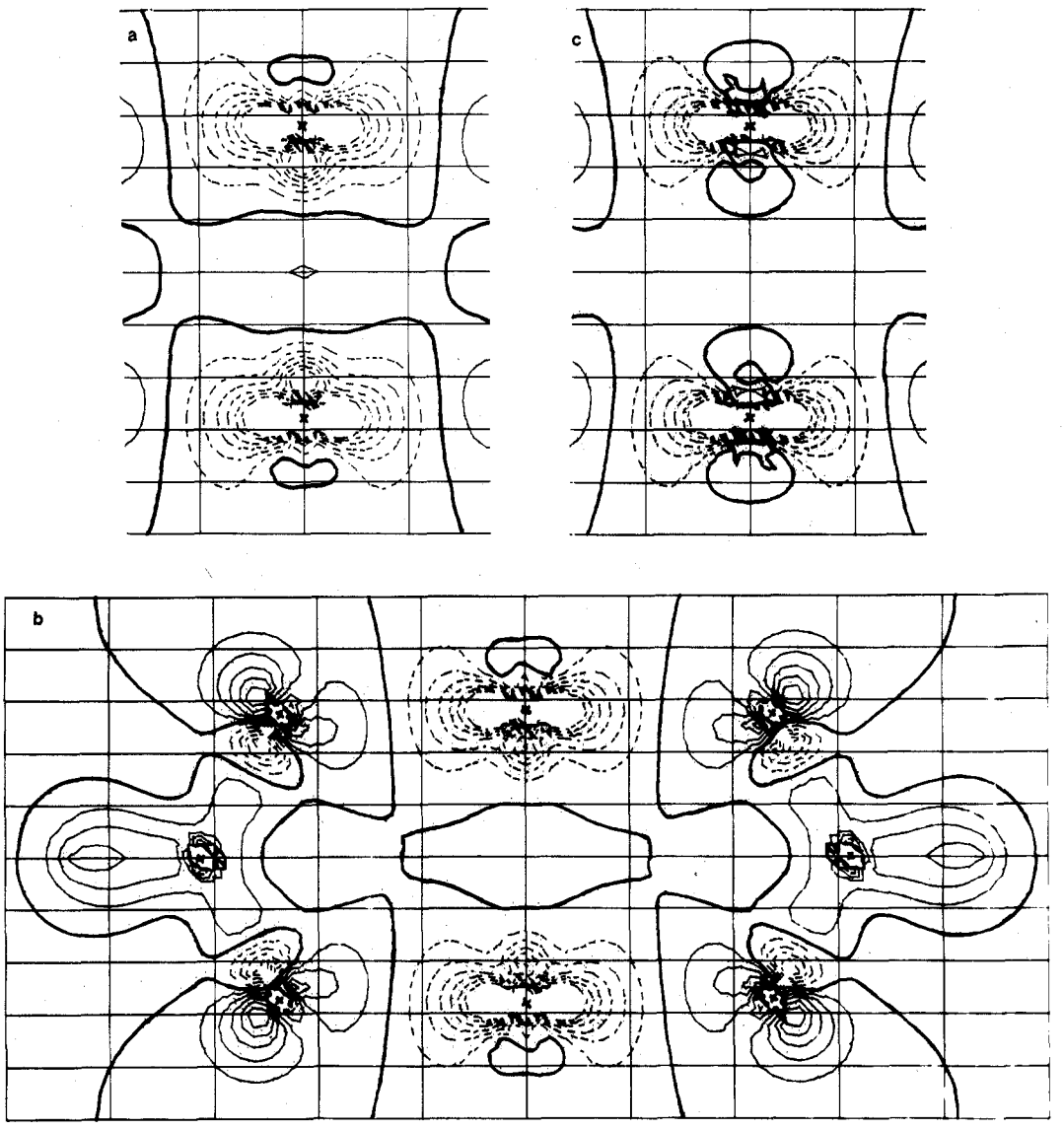

Figure 7. Theoretical density maps in plane I (=II) (contours are at 0.03 e au^{-3} ($\sim$0.2 e $Å^{-3}$), the bold line is the zero contour, and negative contours are broken): (a) from SCF wave function; (b) from limited CI wave function; (c) from BS wave function. (The densities of parts a and c are almost identical with those of part b outside the Cr–Cr region.)

tributed to the diffuse character of the metal d orbitals, which favors large accumulation regions of low density gradient rather than sharp peaks in limited regions. Thus, the absence of a *sharp* bond peak in the metal–metal bonding region in experimental density maps does not constitute evidence against strong metal–metal bonding. The map obtained from the CI wave function (Figure 7b) still displays excess density in the bonding region, but, consistent with the introduction of antibonding contributions, the value of ρ_{max} has been reduced to 0.1 e $Å^{-3}$, and the area of the positive region has become significantly smaller.

Both SCF and CI maps display minima at about 0.30 Å from the Cr atoms in the direction of the center of symmetry. These minima are quite similar to the negative areas observed on the experimental maps in the bonding region. Since the electron population of the individual bonding d orbitals changes little from the atom to the different molecular wave functions,[32] both the minima near the metal atoms and the excess density at the center of the bonding region could be attributed to a charge transfer from the internal to the diffuse component of the double-ζ d_{z^2} orbital. This rationalization also accounts for the two other minima which are observed still on the Cr–Cr axis, but on the external side of the metal atoms, and which probably represent the symmetric deformation of the nonoverlapping lobes of the d_{z^2} orbitals. However, these minima are hardly visible on the third theoretical map, corresponding to the BS wave function (Figure 7c). In that map, the large accumulation zone in the region of the metal–metal bond does not exist anymore and has been replaced with two small positive zones, centered at about 0.5 Å from the Cr atoms, with $\rho_{max} < 0.1$ e $Å^{-3}$. This BS wave function probably corresponds to a further step in the process of localizing d orbitals on individual metal atoms. This is illustrated by the overall metal–metal overlap population, which drops from 0.64 for the SCF configuration to 0.08 for the BS wave function. Quite consistently, this wave function does not yield any visible density deformation with respect to the spherical atoms in the whole region of the metal–metal bond.

The maps obtained from the CI wave function (Figures 7b and 8b) are in several aspects similar to the experimental map reproduced in Figure 5. However, some disagreement is observed in the region of the center of symmetry of the system. The experimental map displays in this region a slightly negative channel separating two large and diffuse excess density regions. However, the positive region in the computed map is continuous and displays a broad maximum ($\rho_{max} = 0.1$ e $Å^{-3}$) around the center of symmetry. Although the differences are quantitatively small (<0.15 e $Å^{-3}$), they are qualitatively important

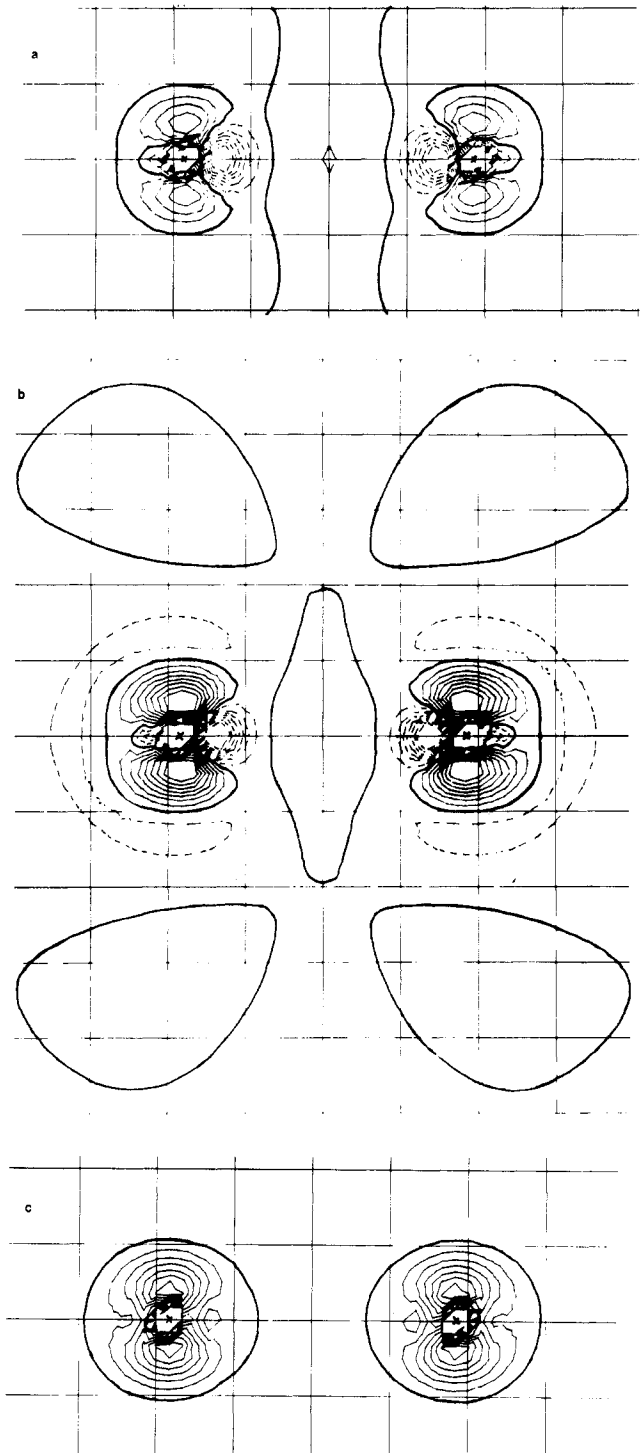

Figure 8. Theoretical density map in plane IV (=V) (a, b, and c as in Figure 7). Contours in parts a and c are at 0.03 e au^{-3} and those in part b are at 0.015 e au^{-3}. Note the accumulation of density in the d_{xy} region around the metal atom which is consistent with the d_{xy} population of 1.069 e, compared with 1.0 e in the ground-state chromium atom.

in the region of the metal–metal σ bond. A tentative explanation may be based on the fact that the crystal used in the experimental investigation is the dihydrated form of dichromium tetraacetate. The sensitivity of the Cr–Cr bond length in dichromium tetracarboxylates to the presence and to the nature of an axial ligand has been extensively documented by Cotton and co-workers (see for instance ref 10). Though the electronic effect of the axial ligands on the chromium–chromium bond is probably overemphasized by a very broad and shallow potential curve,[18,20] its result is a weakening of the bond very probably induced by an interaction between the lone pair of the axial ligand and the d_{z^2} orbitals of chromium. Such an interaction could consistently erase the peak of 0.1 e Å^{-3} obtained at the center of symmetry for the isolated $Cr_2(O_2CH)_4$ system.

Conclusion

It is of interest that almost all binuclear complexes studied so far are characterized by an absence of sharp and definite density peaks in the bonding region.[33] However, this usual lack of really significant accumulation of density might originate from different factors according to the type of the complex. In the case of bis(dicarbonylcyclopentadienyliron) investigated by Mitschler, Rees, and Lehmann[27] ab initio calculations at the SCF level indicate that there is apparently no net direct bonding between the iron atoms.[28] The present study of $Cr_2(O_2CCH_3)_4$ shows that the large zones of very weak density accumulation found in the regions of π and δ bonding agree with the theoretical description of a quadruple bond weakened by large contributions from antibonding configurations. Although the strongly bonded SCF configuration does not give in this case a realistic picture of the metal–metal interaction, it is of interest that the theoretical map obtained from this wave function does not display the sharp peaks which might have been expected. Though the excess density regions are consistently more extended than those obtained from both the experiment and the correlated wave functions, the value of ρ_{max} culminates at 0.2 e Å^{-3} only. This result might denote a specific character of interacting d orbitals. It could be used to explain the lack of significant accumulation of density observed in the case of complexes which are expected to display normal metal–metal bonds; for instance μ-octatetraenyl-bis(cyclopentadienylchromium)[29] and the nonbridged manganese decacarbonyl.[30,34]

Acknowledgment. The authors thank Dr. D. F. Chodosh for synthesis of the title compound. Financial support of this work by the National Science Foundation (Grant CHE 7613342A01) is gratefully acknowledged. Molecular orbital calculations have been carried out at the Centre de Calcul du C.N.R.S. in Strasbourg-Cronenbourg. We thank the staff for their cooperation.

Registry No. $Cr_2(O_2CCH_3)_4 \cdot 2H_2O$, 14404-41-2.

(26) Wang, Y.; Coppens, P. *Inorg. Chem.* **1976**, *15*, 1122.
(27) Mitschler, A.; Rees, B.; Lehmann, M. S. *J. Am. Chem. Soc.* **1978**, *100*, 3390.
(28) Benard, M. *Inorg. Chem.* **1979**, *18*, 2782.
(29) Gerbel, W.; Wilke, G.; Goddard, R.; Kruger, C.; Mynott, R. *J. Organomet. Chem.* **1978**, *160*, 139.
(30) Rees, B., private communication.
(31) Heyser, W. Thesis, Free University, Amsterdam, 1979; *Int. J. Quantum Chem.* **1978**, *S12*, 169.
(32) The atomic configuration of chromium is d^5s^1, thus yielding an average population of 1 to each d orbital. As a comparison, the populations of the d_{z^2} (σ), d_{xz} (π) and d_{xz} (δ) orbitals are 0.934, 1.010, and 1.069, respectively, on each chromium atom for the SCF configuration. For the BS configuration, the corresponding populations are 0.983, 1.014, and 1.024.
(33) μ-Acetylene-bis(cyclopentadienylnickel) for which a large peak was found between the nickel atoms, represents an exception.[26] However, this last observation is at variance with calculations at the SCF level[8] which indicate most of the region between the metals to be one of electron deficiency. It is not known to what extent this disagreement is due to experimental error (the structure is acentric, which increases experimental uncertainty) or to the neglect of configuration interaction in the calculation.
(34) Some bonding density was found, however, in theoretical maps displaying the deformation density of $Mn_2(CO)_{10}$ with regard to the $Mn(CO)_5$ fragments.[31]